

Supporting Information for:

Enhanced Activity and Stability of Organophosphorus Hydrolase via Interaction with an Amphiphilic Polymer

Minkyu Kim,[†] Manos Gkikas,[†] Aaron Huang,[†] Jeon Woong Kang[§], Nisaraporn
Suthiwangcharoen[‡], Ramanathan Nagarajan[‡] and Bradley D. Olsen^{*,†}

[†]Department of Chemical Engineering, Massachusetts Institute of Technology, Cambridge, MA,
02139

[§]Laser Biomedical Research Center, G. R. Harrison Spectroscopy Laboratory, Massachusetts
Institute of Technology, Cambridge, MA, 02139

[‡]Molecular Sciences and Engineering Team, Natick Soldier Research, Development &
Engineering Center, Natick, MA, 01760

*E-mail: bdolsen@mit.edu

Materials and Methods

Materials. Paraoxon-methyl, Pluronic F127 and Poly(ethylene glycol) were purchased from Sigma-Aldrich (product # 46192, p2443 and 202444). F88 and P123 were purchased from BASF (product # 30085864 and 30085707). 3:1 and 0.33:1 (PEO:PPO wt ratio) diblock copolymers were purchased from Polysciences, Inc. (product # 16276 and 16274).

DNA engineering and OPH expression and purification. A gene sequence encoding for organophosphate hydrolase (OPH) from serine 30 of the opd gene, proposed open reading frames,¹ was purchased (GenScript, USA) and subcloned into a pET15b expression plasmid (Novagen, USA) through NdeI and BamHI restriction sites. To increase solubility of OPH enzymes and activity for paraoxon hydrolysis, multiple single-site mutations were incorporated using a commercial site-directed mutagenesis kit (product # 210515, Agilent, USA): K185R and I274N for the OPH catalytic activity,² and K185R, D208G and R319S for the improved soluble OPH yields during expression.³ The primers were K185R, 5'- T CAG GAA CTG GTT CTG CGT GCA GCT GCG CGT GCG -3', D208G, 5'- GCC GCA AGT CAA CGT GGC GGT GAA CAG CAA GCT G -3', I274N, 5'- TCT GCT CTG CTG GGT AAC CGT TCG TGG CAG ACC -3' and R319S, 5'- ATG GAT GTG ATG GAC AGC GTT AAT CCG GAT GG -3'. The PCR fidelity of the mutated plasmid was confirmed by the gene sequencing (Genewiz, USA).

A freshly grown bacterial colony was inoculated in 5ml LB medium supplemented with 1 mM ampicillin at 37°C overnight. For pre-culture, 1 L LB medium with 1 mM ampicillin and 5 ml of the overnight culture were incubated until an OD₆₀₀ of ~0.4 at 30°C. Then, OPH enzymes were expressed for 21 hours at 30°C in the presence of 0.5 mM IPTG and 1 mM CoCl₂. Cells containing enzymes were harvested by spinning down at 4,000 g for 10 min, and then

precipitated cells were stored at -80°C. Frozen cells were resuspended in lysis buffer containing 10 µg/mL DNase, 20 µg/mL RNase A, 50 mM NaH₂PO₄, 300 mM NaCl and 5 mM imidazole (pH ~8) at 4°C and then lysed by the sonication. After spinning down the lysates at 14,000 g for 30 min at 4°C, His₆-tagged OPH enzymes in supernatants were purified by cobalt affinity columns (product # 89965, Thermo Scientific, USA) at 4°C. The purified enzyme was then chromatographed using a HiTrap Q HP column (product # 17-1154-01, GE Healthcare, Uppsala, Sweden) in an AKTA FPLC machine. OPH enzymes were dialyzed into the OP testing buffer, containing 40 mM HEPES (pH 8), 100 mM NaCl and 0,1 mM CoCl₂. Yields of 20~30 mg/L were obtained as estimated using the BCA protein assay kit (product # 23227, Thermo Scientific, USA). Enzymes were determined to be greater than 95% pure by SDS-PAGE analysis (inset of Figure 2a). Except where otherwise noted, the OP testing buffer was used for all testing, and sample storage.

Circular Dichroism (CD) spectroscopy. An Aviv model 202 CD spectrometer recorded far UV CD spectra. The spectra were recorded in a 0.1 cm path length cuvette at a scan rate of 12 nm/min. Enzyme samples (0.25 mg/mL) were measured in 20 mM Tris (pH 8), 100 mM NaCl and 0.1 mM CoCl₂ in the presence or absence of 20 % MeOH. The CD signal, after the buffer signal subtractions, was converted into mean residue ellipticity (MRE), calculated by $[100 \cdot \text{observed ellipticity (deg)}] / [\text{path length (cm)} \cdot \text{enzyme concentration (M)} \cdot \text{total number of amino acids per enzyme}]$.

UV-Vis spectroscopy. A Varian Cary 50 Bio UV/visible spectrophotometer with temperature controller (TC125, Quantum Northwest, USA) was used to measure the OPH activity at 25°C.

Paraoxon-methyl was diluted to 0.2-0.7 mM in the OP testing buffer. In each 1 ml test volume, 0.05 - 0.2 $\mu\text{g/ml}$ of OPH enzyme and 0.1 mM of paraoxon with various concentrations of polymers were mixed in a 1 cm path length methacrylate cuvettes (product # 14-955-128, Fisher Scientific, USA). The activity was measured by the absorbance of the hydrolysis product of paraoxon, p-nitrophenol, at a wavelength of 405 nm.

MALDI-TOF spectroscopy. A Bruker Daltonic Microflex mass spectrometer MALDI-TOF was used with the linear positive method for proteins. Samples were diluted to 10 mg/ml of OPH and 5mg/ml of Pluronic before being deposited onto the target. Sinapinic acid was used as a matrix.

NMR spectroscopy. ^1H NMR spectroscopy and NOESY 2D-NMR (500 MHz) were acquired using a VARIAN Inova-500 NMR spectrometer with an Oxford Instruments Ltd. superconducting actively-shielded magnet with quad broadband RF (4 with Wave Form Generation). The spectra were acquired at room temperature in 90% HEPES buffer and 10% D_2O under saturating conditions.

Raman spectroscopy. The Raman system used for these experiments is described in detail elsewhere.⁴ A 785 nm wavelength Ti: Sapphire laser (3900S, Spectra-Physics) pumped by a frequency-doubled Nd: YAG laser (Model Millennia 5sJ, Spectra-Physics) was used for the excitation. A 1.2 NA water immersion objective lens (Olympus UPLSAPO60XWIR 60X/1.20) was used both to focus the laser onto the sample and to collect the backscattered light. The collected signal was filtered and delivered to a spectrograph (Holospec f/1.8i, Kaiser Optical Systems) and detected by a TE-cooled, back-illuminated, deep depleted CCD (PIXIS:

100BR_eXcelon, Princeton Instruments). The laser power was measured at the sample to be ca. 20 mW and integration time was 10 seconds. Background signals from acquired Raman spectra are processed by Lieber fitting with a 5th-order polynomial.⁵

Briefly, this algorithm removes slowly varying background while maintaining narrow Raman peaks. A well-known potential issue for this background removal process is that slowly varying background signal can be removed differently from each spectrum. Therefore, for quantitative analysis, Raman peaks, especially the area under the peak on top of broad background signal, are compared to other Raman peaks. In this study, the peak area in the 1650 cm⁻¹ Raman band was selected to normalize other peaks. The 1650 cm⁻¹ band represents amide bonds that are existed in polypeptide but not existed in the polymer and the buffer contents as shown in Figure S6. After the normalization of known Raman signals from proteins⁶, the peak differences between OPH solution and OPH/Pluronic mixture were compared as follows:

Raman bands	Area under the peak differences (%)
1004 Phe symmetric ring breath	12.4 %
1033 Phe C-H in-plane	12.87 %
1209 Phe C-C ₆ H ₅ stretching, Trp	12.36 %
1257 amide III	-0.39 %
1320 protein C-H deformation	0.16 %
1450 protein & lipid CH deformation	-0.98 %

Although similar % of peak differences in Phe and Trp in other known Raman bands were observed compared to the 1004 cm⁻¹ Raman band, their signal to noise ratios were not strong (Figure 2c). On the other hand, Phe Raman signal at 1004 cm⁻¹ was strong (Figure 2c); thus, it was clear to identify the 12 % reduction of the OPH/Pluronic Raman peak compared to the OPH peak, suggesting the interaction between the polymer and the enzyme.

Fluorescence spectroscopy. Fluorescence spectra of OPH, Pluronic and OPH/Pluronic were measured with a Fluorolog-3 spectrophotometer (Horiba Jobin Yvon, New Jersey, USA) in 10 mm path-length NSG Precision Cells quartz cuvettes (New York, USA). For the emission experiments, spectra were taken in 1 nm steps at a fixed excitation wavelength of 280 nm. Slits were adjusted to 5nm bandwidth for both excitation and emission.

OPH activity and efficiency. The activity was determined by calculating the initial slope of the UV-vis traces. The absorbance was then converted to concentration using the extinction coefficient of $16.2 \text{ mM}^{-1} \cdot \text{cm}^{-1}$ to determine the rate of substrate conversion.

Because of the finite mixing time involved in the measurement, in most cases, activity was compared using k_{cat}/K_M ^{7,8} (Figure 1 and Figure 3), a term commonly known as enzymatic efficiency. The enzymatic efficiency was calculated with the catalytic constants k_{cat} and K_M estimated by fitting time-course data from UV-Vis spectroscopy to the Schnell-Mendoza solution of the Michaelis-Menten equation as follows:⁹

$$\frac{[S]}{K_M} = \omega \left[\frac{[S]_0}{K_M} \exp \left(\frac{[S]_0}{K_M} - \frac{[E] \times k_{\text{cat}} t}{K_M} \right) \right]$$

where ω is the Lambert function, $[S]$ is the substrate concentration, $[S]_0$ is the initial substrate concentration, $[E]$ is the enzyme concentration, K_M is the Michaelis constant, k_{cat} is the turnover number, and t is time. For this calculation, the extinction coefficient for the analyte in the OP testing buffer at 25°C was measured via calibration with *p*-nitrophenol (product # 241326, Sigma-Aldrich, USA) to be $\epsilon_{405\text{nm}} = 16200 \text{ M}^{-1} \text{ cm}^{-1}$, and the initial concentration of paraoxon-methyl was taken as the concentration of the analyte at complete hydrolysis. Enzymatic efficiency⁷ was chosen over activity because of the difficulty of accurately measuring activity under our experimental conditions. Due to the low concentrations of our enzyme and substrate,

the low solubility of the substrate, the instability of the enzyme, and the high rate of the reaction relative to the mixing time at the start of our reaction, a smaller error bound in measurements of kinetic efficiency. The calculated values for the kinetic parameters for fresh OPH (less than a week after cell lysis) were as follows: $k_{\text{cat}} = 2900 \pm 400 \text{ s}^{-1}$ (mean \pm standard deviation) and $k_{\text{cat}}/K_{\text{M}} = 36000 \pm 5000 \text{ mM}^{-1}\text{s}^{-1}$. These values are comparable to those found in literature.^{7,10}

Paraoxon solubility estimation. Paraoxon-methyl solubility in water was estimated using Estimation Program Interface (EPI) Suite v4.11 using SMILES notation c1(OP(=O)(OC)(OC)ccc(N(=O)=O)cc1. This yielded an estimated water solubility of 731 mg/L. This estimate was tested by making a mixture of this concentration. After brief mixing, the mixture appeared homogeneous.

References

- (1) Mulbry, W. W.; Karns, J. S. *J Bacteriol* **1989**, *171*, 6740.
- (2) Cho, C. M. H.; Mulchandani, A.; Chen, W. *Protein Eng Des Sel* **2006**, *19*, 99.
- (3) Roodveldt, C.; Tawfik, D. S. *Protein Eng Des Sel* **2005**, *18*, 51.
- (4) Kang, J. W.; Lue, N.; Kong, C. R.; Barman, I.; Dingari, N. C.; Goldfless, S. J.; Niles, J. C.; Dasari, R. R.; Feld, M. S. *Biomed Opt Express* **2011**, *2*, 2484.
- (5) Lieber, C. A.; Mahadevan-Jansen, A. *Appl Spectrosc* **2003**, *57*, 1363.
- (6) Chan, J. W.; Lieu, D. K.; Huser, T.; Li, R. A. *Anal Chem* **2009**, *81*, 1324.
- (7) Komives, C. F.; Lilley, E.; Russell, A. J. *Biotechnol Bioeng* **1994**, *43*, 946.
- (8) Raushel, F. M. *Curr Opin Microbiol* **2002**, *5*, 288.
- (9) Schnell, S.; Mendoza, C. *J Theor Biol* **1997**, *187*, 207.
- (10) Shimazu, M.; Mulchandani, A.; Chen, W. *Biotechnol Bioeng* **2003**, *81*, 74.

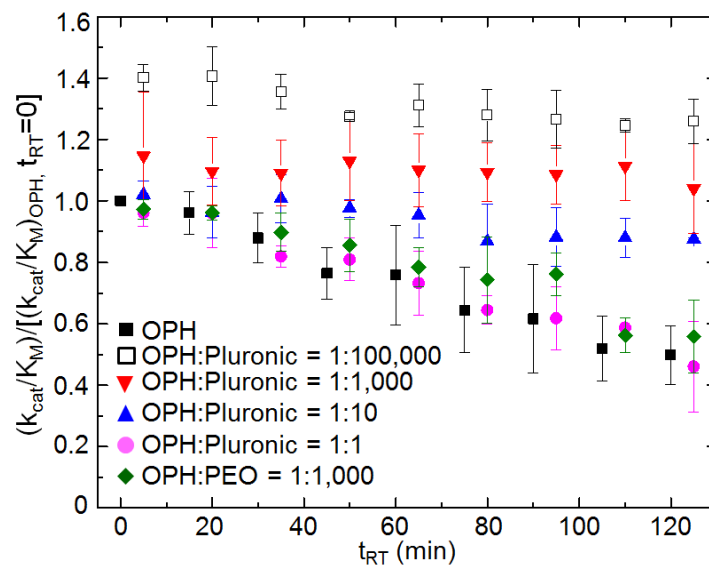


Figure S1. The enzymatic efficiency comparisons (with standard deviations) of OPH with different molar ratios of Pluronic and PEO over time of OPH with varying molar ratios of Pluronic and PEO polymers ($n=6$ for OPH and $n=3$ for others).

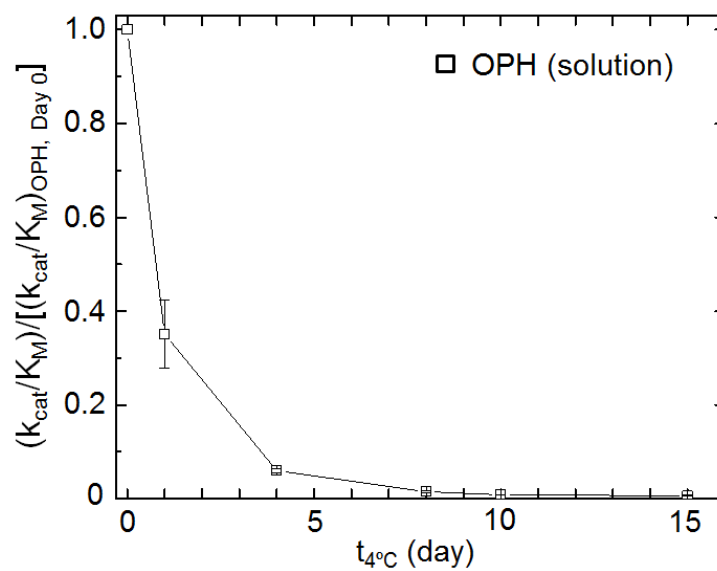


Figure S2. Relative activity measurements of OPH stored in solution, containing 40 mM HEPES (pH 8), 100 mM NaCl and 0.1 mM CoCl_2 , at 4°C ($n = 3$). Paraoxon degrading activity was measured at 25°C . The OP degrading activity was taken relative to the activity of OPH on day 0.

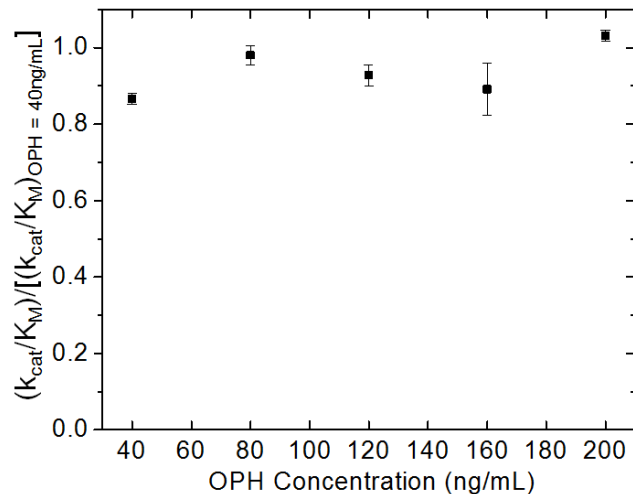


Figure S3. Relative activity of OPH at various concentrations. The kinetic efficiency values for each test are presented relative to the kinetic efficiency of a 40 ng/mL sample taken immediately before each test to account for any loss of enzymatic activity as a function of time as the tests were performed. Relatively constant activity as a function of concentration indicates that OPH solubility is not a concern at the concentrations tested in this experiment.

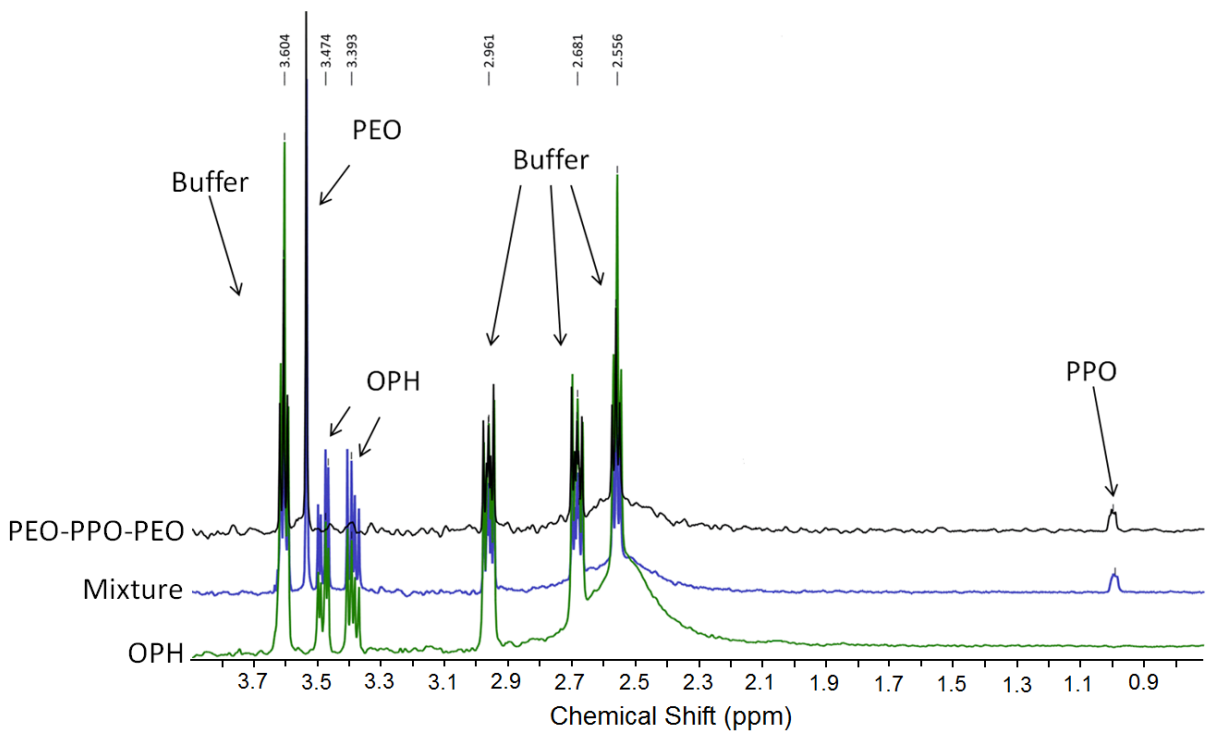


Figure S4. ¹H NMR spectrum of Pluronic (PEO-*b*-PPO-*b*-PEO), OPH and OPH/Pluronic mixture at saturating conditions: 90% HEPES buffer/10% D₂O, molar ratio OPH/Pluronic = 1:1.

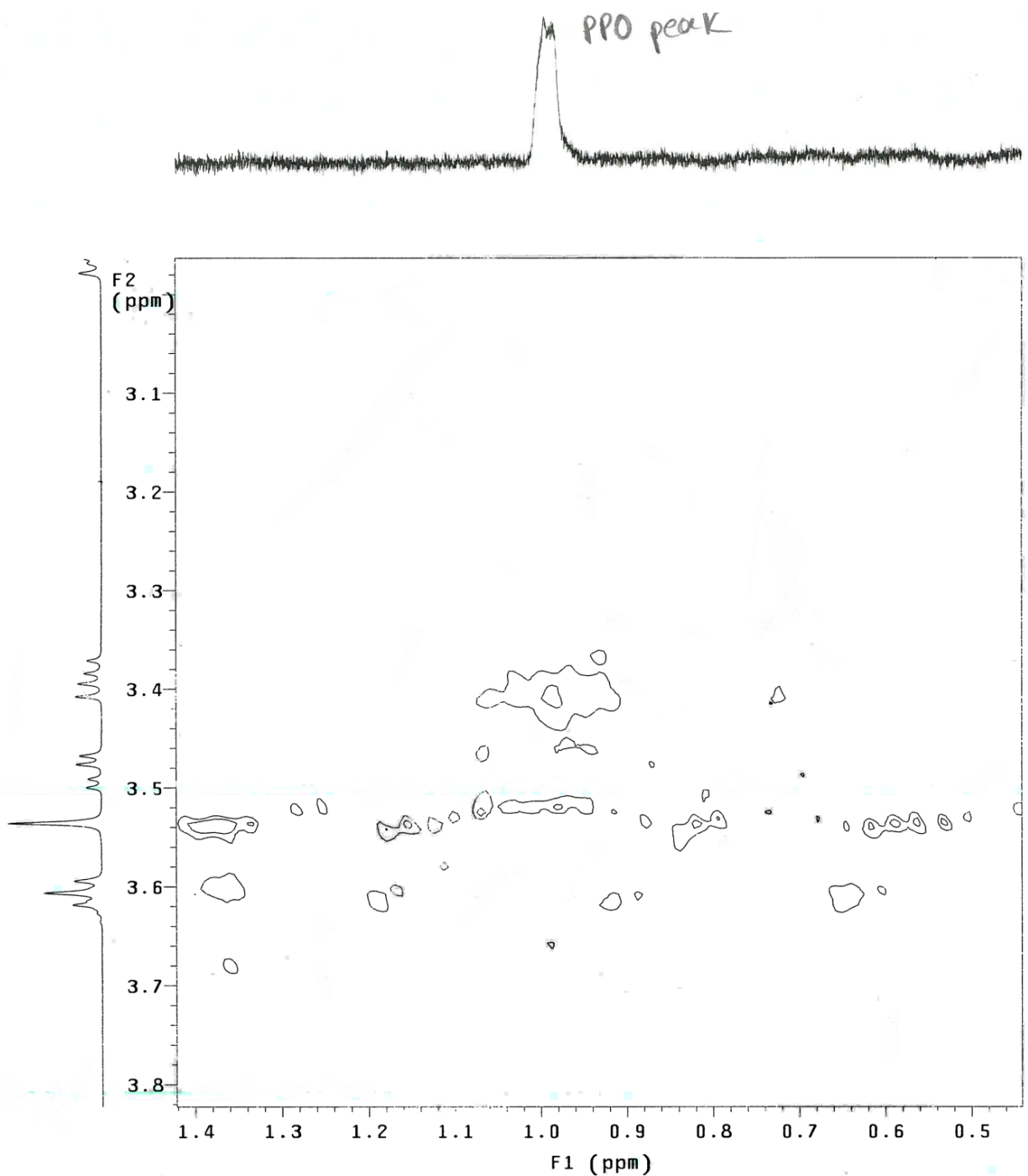


Figure S5. 2D NOESY spectrum of OPH/Pluronic mixture at saturating conditions (90% HEPES buffer/10% D₂O, molar ratio OPH/Pluronic = 1:1) showing the correlation of the PPO peak with the enzyme peak at 3.4 ppm.

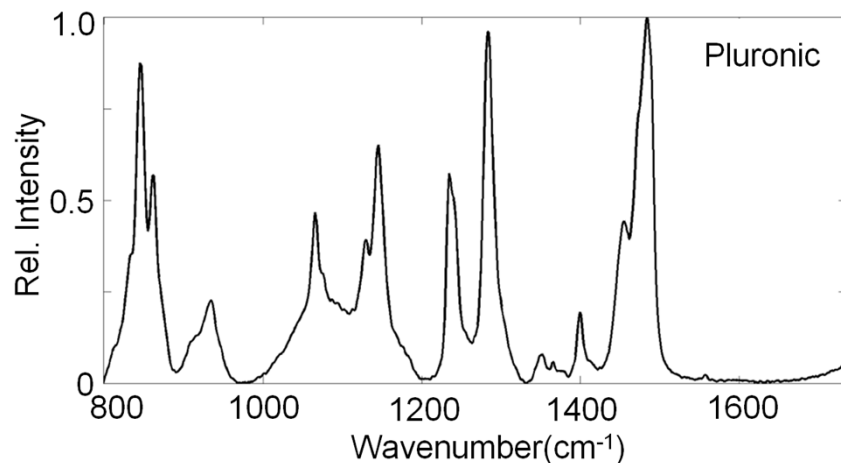


Figure S6. Raman spectrum of Pluronic in dried form. Raman signal at 1650 cm^{-1} which represents amide band I is selected to normalize both Raman spectra of OPH and OPH/Pluronic mixture (Figure 2c). To confirm that there is no Raman signal/peak from either Pluronic or the buffer contents (40 mM HEPES (pH 8), 100 mM NaCl and 0.1 mM CoCl_2), samples with the buffer were deposited on the substrate and dried (drop-coating deposition Raman spectroscopy). Since Pluronic and the buffer contents do not have any Raman signal at 1650 cm^{-1} , the normalization of the spectrum at this wavenumber for both OPH and OPH/Pluronic mixture is applicable. In this figure, the spectrum was normalized by maximum intensity at around 1480 cm^{-1} .

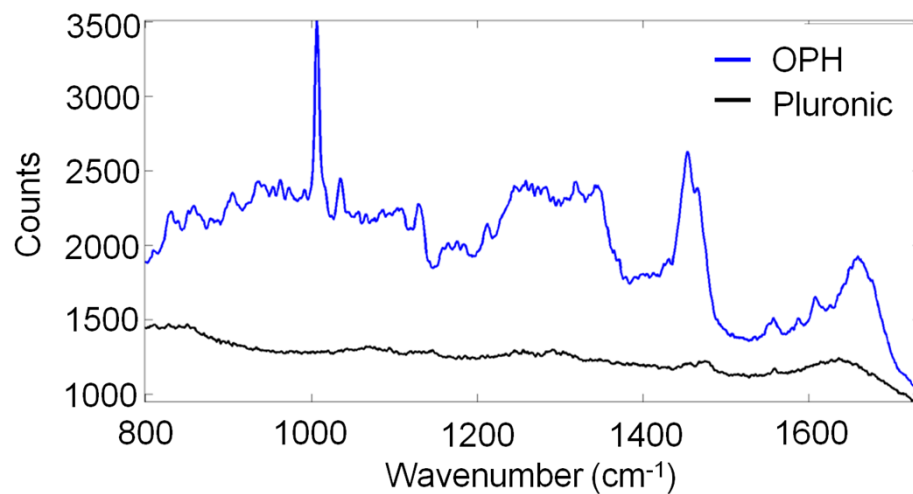


Figure S7. Comparison of raw Raman spectra of OPH and Pluronic, measured in the OP testing buffer.

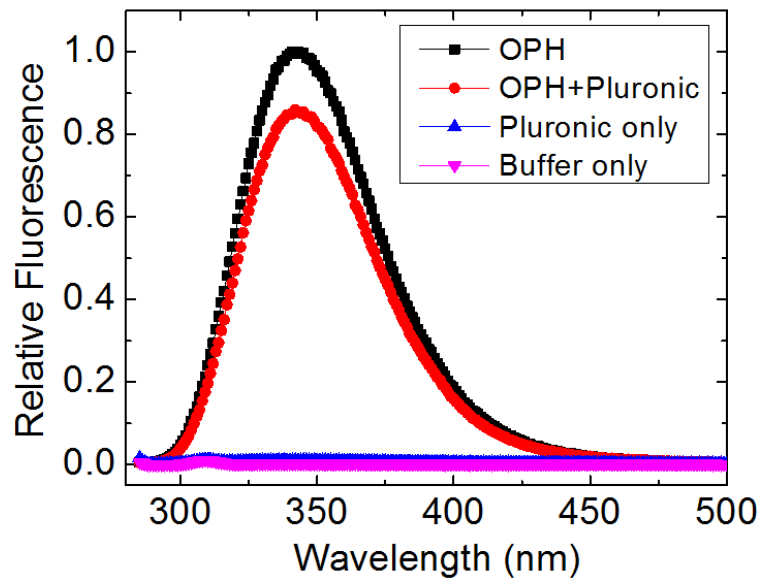


Figure S8. Tryptophan fluorescence spectra of OPH enzymes in the absence and presence of Pluronic. OPH sample contains 1 mg/mL OPH with 40 mM Hepes (pH 8), 100 mM NaCl and 0.1 mM CoCl_2 . The addition of Pluronic (5 mg/mL concentration) into the OPH sample caused a 15.8% decreasing in the Trp fluorescence intensity at 355 nm compared to OPH sample without Pluronic, suggesting that Trp hydrophobic amino acids of OPH interact with Pluronic.

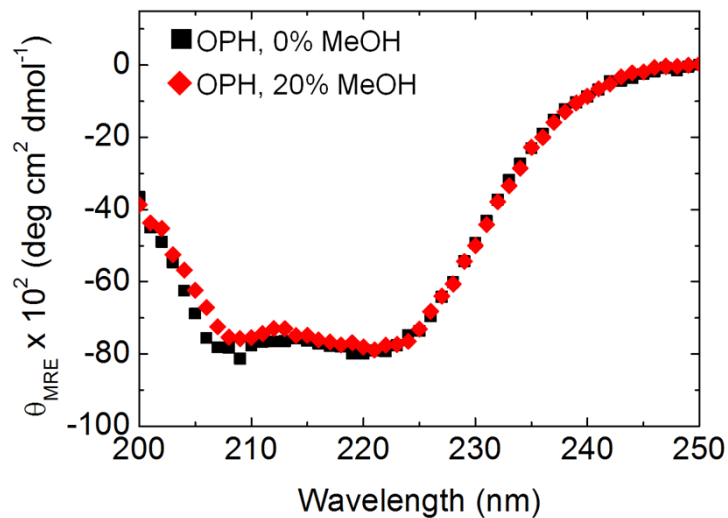


Figure S9. CD spectra of OPH enzymes in the absence and presence of 20 % MeOH. In addition to MeOH, sample contains 0.25 mg/mL OPH with 20 mM Tris (pH 8), 100 mM NaCl and 0.1 mM CoCl₂. 20% (v/v) MeOH does not result in measurable changes in the OPH secondary structure. This suggests that MeOH do not significantly denature OPH but instead quench the active site of OPH, resulting in a decrease in the OP degrading activity (Figure 3a).

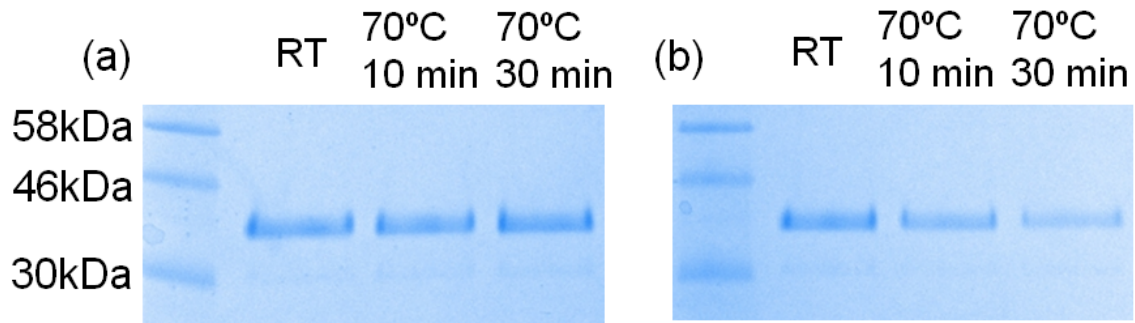


Figure S10. OPH aggregation by high heat exposure. SDS-PAGE results show that the OP degrading activity of OPH at high heat exposure results in part due to OPH aggregation. OPH (1mg/mL) were prepared and exposed to 70 ± 3 °C. After the exposure, the samples were centrifuged for 5 min at 4 °C at 21xg (a) samples before centrifugation after the heat exposure showing total protein and (b) supernatants after the centrifugation showing soluble protein. The loss of soluble protein during heat treatment is suggestive of aggregation.

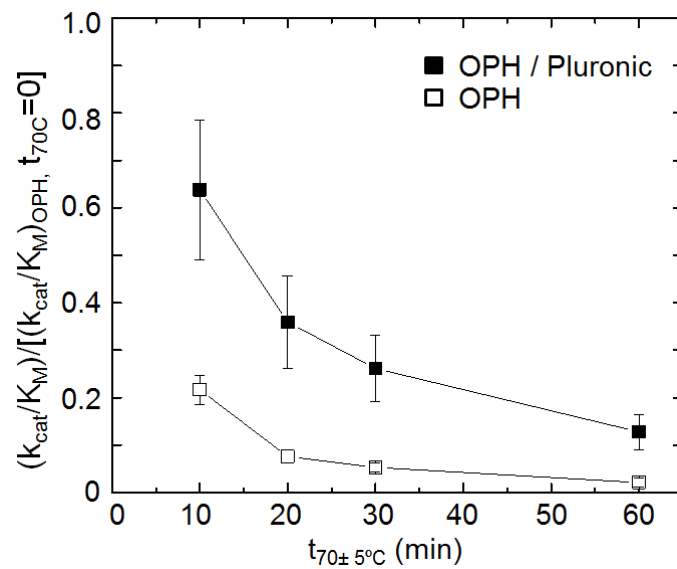


Figure S11. Relative activity measurements of OPH and OPH/Pluronic mixtures (1:1000 molar ratio) at high temperatures ($n=3$). Both samples were exposed at $70\pm 5^\circ C$ with a prescribed amounts of time ($t_{70\pm 5^\circ C}$) and paraoxon degrading activity was measured at $25^\circ C$.

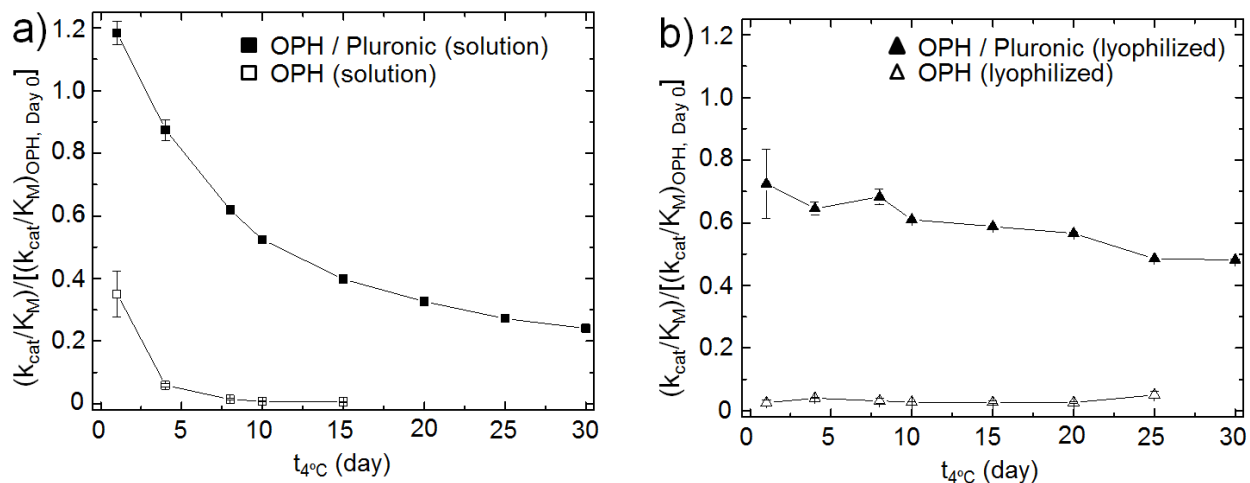


Figure S12. Relative activity measurements of OPH and OPH/Pluronic mixtures (1:1000 molar ratio), stored in solution (a) and in the lyophilized form (b). 50 ml of OPH (0.2 $\mu\text{g}/\text{ml}$) and 50 ml of OPH/Pluronic mixtures were prepared in the OP testing buffer and half of each sample were lyophilized in day 0. All prepared samples in solution and in the lyophilized form were stored at 4°C. Upon hydration of lyophilized samples after a prescribed storage period ($t_{4^\circ C}$), all four samples, OPH and OPH/Pluronic from the solution (a) and the lyophilized form (b), were diluted five times and paraoxon degrading activity was measured at 25°C ($n = 2$ or 3). The OP degrading activity was taken relative to the activity of OPH in the absence of Pluronic on day 0.

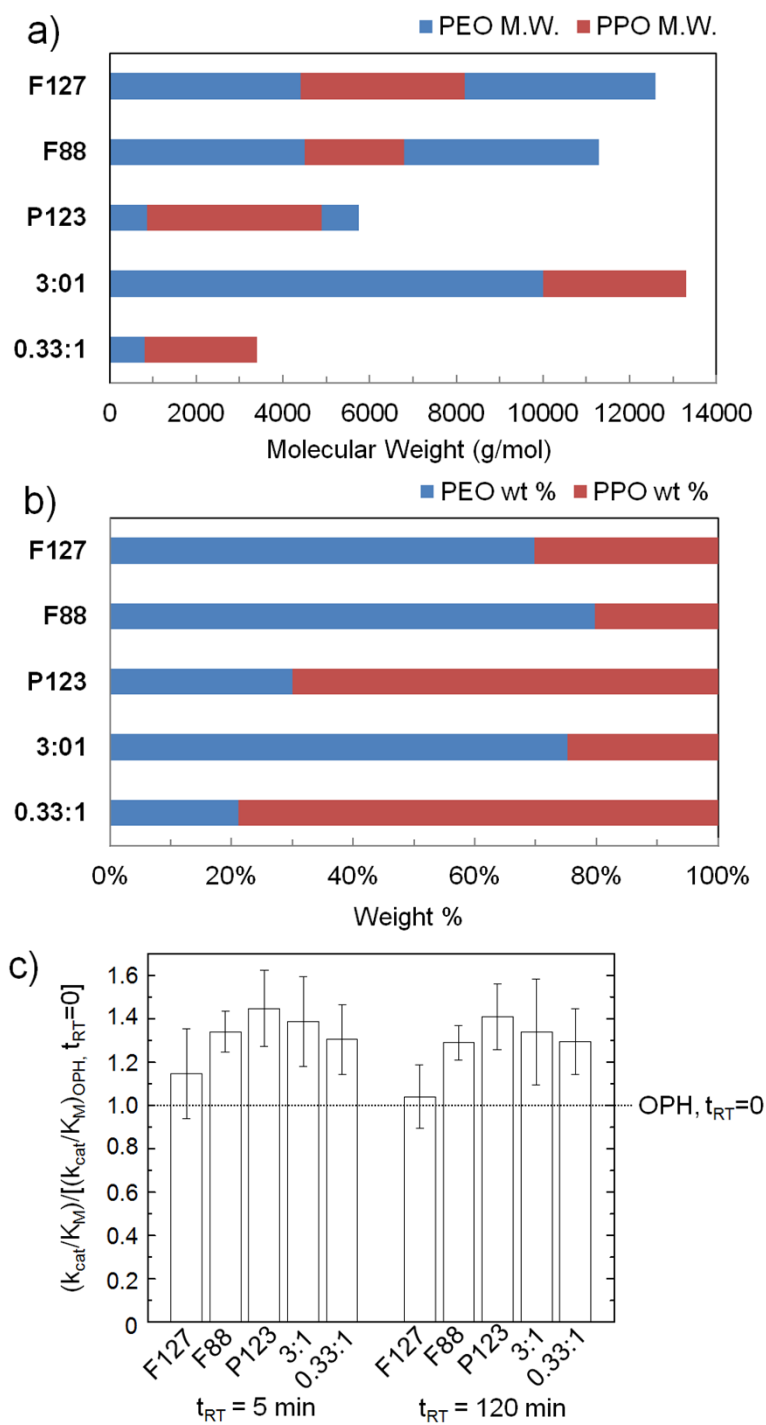
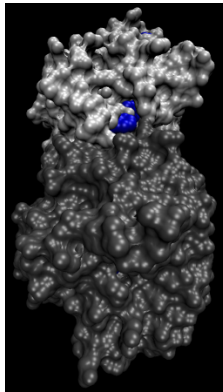
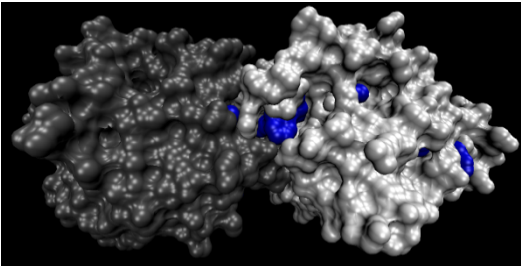
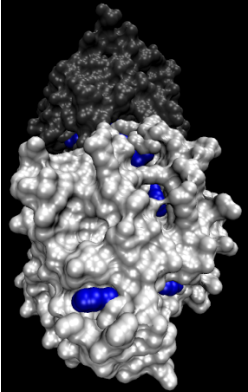
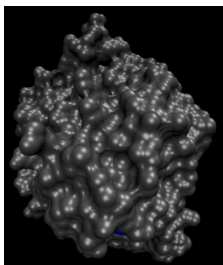
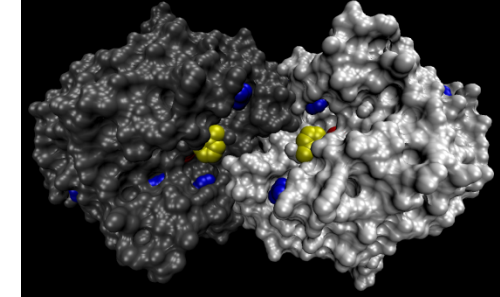
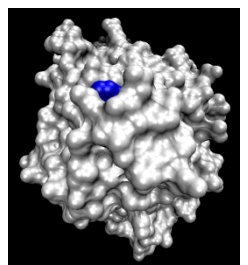
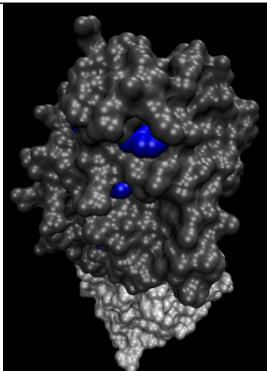
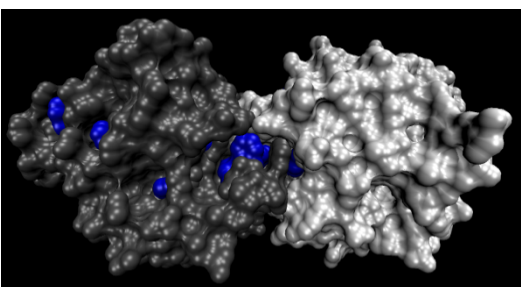
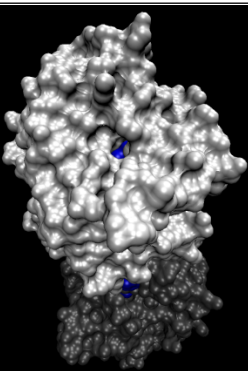


Figure S13. Effects of PEO-*b*-PPO-*b*-PEO triblock (Pluronic F127, F88, P123) and PEO-*b*-PPO diblock (3:1, 0.33:1) copolymers on OPH stability and detoxification activity. To understand whether i) the polymers containing the PPO block, ii) wt % of PPO blocks and iii) different types of block copolymers can affect the OPH stability and the activity, OPH and various polymers (a,

b) were blended in 1:1000 molar ratio and the OP detoxification activities were measured. Each set of experiments, including OPH as the internal standard and OPH/polymer mixtures, was separately prepared and the activity was measured 3 times (n=3 for each polymer). Compared to OPH alone, OPH/polymer mixtures showed higher activity and stability over 2 hours at RT (c). While a wide variety of diblock and triblock copolymers containing PPO blocks enhance the detoxification activity and stability of OPH, the changes in molecular design do not show statistically significant differences compared to Pluronic F127 under the conditions tested ($P>0.05$).

Table S1. Locations of Phe residues on the OPH surface. Side chains of Phe (F) residues are depicted as blue and yellow. To clearly indicate the OP catalytic sites in the OPH dimer, F132 residues located in the catalytic sites of each monomer are illustrated as yellow. OPH monomers are colored as gray and white to clearly illustrate the dimeric nature of the active form.

	Left	Middle	Right
Top			
Front			
Bottom			
Back		